

UNIVERSITÄT BONN  
Physikalisches Institut



Performance of a beam telescope  
using double sided silicon microstrip detectors<sup>\*</sup>

SW 95 30

P. Fischer<sup>a</sup>, R. Hammarström<sup>b</sup>, S. Menke<sup>a</sup>, B. Raith<sup>a</sup>,  
O. Runolfsson<sup>b</sup>, N. Wermes<sup>a</sup>

<sup>a</sup> *Physikalisches Institut der Universität Bonn*

<sup>b</sup> *CERN, Geneva, Switzerland*

**Abstract:** A beam telescope consisting of four double sided, DC coupled microstrip detectors with VLSI readout electronics has been built and tested in a 70 GeV  $\mu^-$  beam at CERN. A signal to noise ratio of 53:1 and a spatial resolution of  $2.7\mu\text{m}$  (junction side) and  $4.8\mu\text{m}$  (ohmic side) have been observed on the best detectors. A telescope performance for a particle track of  $\sigma_{xy} = 2 - 3\mu\text{m}$  and  $\sigma_{\text{slope}} = 2 - 3\mu\text{rad}$  on the front face of a test object was achieved.

---

<sup>\*</sup>Work supported by the German Ministerium für Bildung, Wissenschaft, Forschung und Technologie (BMBF) under contracts no. 05 6BN 18P 4 and 05 6BN 10I and by the Ministerium für Wissenschaft und Forschung des Landes Nordrhein-Westfalen under contracts no. IV A5 - 106 001 94 and IV A5 - 9036.0.

Post address:  
Nussallee 12  
D-53115 Bonn  
Germany



BONN-HE-95-01  
Bonn University  
April 1995  
ISSN-0172-8733

# 1 Introduction

Silicon microstrip detectors are used in high energy physics experiments whenever high precision measurements in terms of space resolution are required. Microvertex detectors in collider experiments are examples where high resolution allows precision measurements on the lifetime of fundamental particles by detecting their decay vertex in space [1]. Strip detectors have also been found to be important as beam telescopes determining the position of a high energy particle beam on an event by event basis [2]. So far, mostly single-sided detectors have been used as telescope units. In this paper we report on the assembly and the use of a beam telescope consisting of four stations of double sided microstrip detectors in a CERN high energy muon beam [3].

The beam telescope consists of four independent detector units, the power-supplies and the DAQ system. The setup in the testbeam is shown in fig. 1. A sketch of the layout and the data flow of one unit is shown in fig. 2. Each detector unit consists of a double sided, DC coupled silicon microstrip detector and the front-end electronics, contained in an Al frame housing. For operation, five voltages ( $\pm 7\text{ V}$ ,  $V_{\text{Bias}}$  and  $V_{\text{Bias}} \pm 7\text{ V}$ ) per station are supplied by specially designed power supplies, one supply servicing each unit.

A VME based DAQ system, running the OS9 operating system, consists of a CPU [4], a sequencer module which provides the timing and control signals for the front end electronics and of four 10-bit flash-ADCs [5], one per detector unit.

The specific application for the telescope was to provide accurate knowledge of the entrance point of beam particles on the front face of a Si/W calorimeter [6] under test. The modules no. 1 and no. 2, respectively no. 3 and no. 4 are mounted orthogonally to each other to balance the different intrinsic resolutions of the detector sides due to different readout pitches. Module no. 3 and no. 4 are mounted directly onto the calorimeter face, no. 1 and no. 2 are installed 2 m upstream. The apparatus was installed in the CERN-SPS testbeam using muons of 70 GeV as well as 45 GeV and 22.5 GeV electrons. The results of the calorimeter are not reported in this paper.

## 2 The detector unit

A detector unit contains the double sided strip detector connected via capacitor chips to four readout chips (VIKING [7]) on each side. Capacitor chips ( $\sim 150\text{ pF}$ ) are used to provide AC-coupling between detector strip and preamplifier. The p-side (junction side) strips are wire-bonded directly to the coupling capacitors of the readout lines. The connection of the  $n^+$ -side strips is made using a Z-print which is a glass substrate with

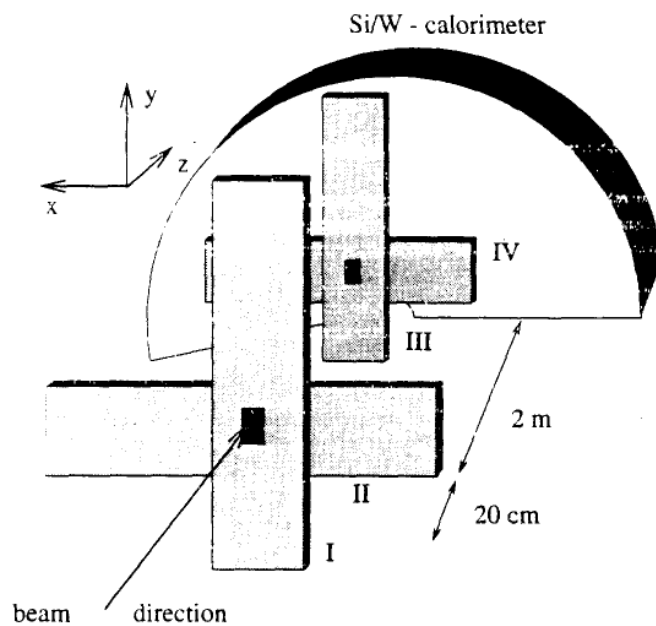


Figure 1: The testbeam setup

printed gold lines connecting all strip contacts to the readout chips. The readout chips receive their control signals from the local sequencer, a FPGA-chip [9]. Readout chips, local sequencer and peripheral electronics are mounted on two ceramics (hybrids). A printed circuit board (interconnect card) serves as interface between detector unit and the rear end readout electronics.

The detectors are double sided, DC coupled silicon  $\mu$ -strip detectors manufactured by CSEM [8]. They are made from high resistivity ( $\sim 10 \text{ k}\Omega\text{cm}$ )  $280 \mu\text{m}$  thick n-doped silicon wafers. Each detector has an active area of  $7.04 \times 3.84 \text{ cm}^2$ .

The junction side strips ( $\text{p}^+$ -strips) are biased via the punch through current effect. The

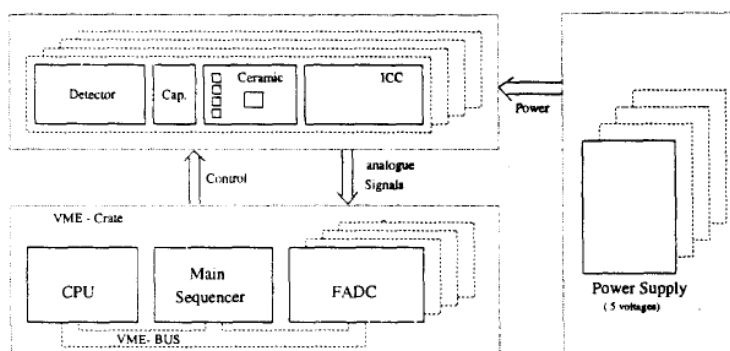


Figure 2: A block diagram of the testbeam telescope

effective bias resistance is  $\sim 2.2 \text{ G}\Omega$  depending on the single strip leakage current which is in the order of  $50 - 150 \text{ pA}$ . The implant strip pitch is  $25 \mu\text{m}$ , while the readout pitch is  $50 \mu\text{m}$ . The information from intermediate strips is used through capacitive coupling between strips.

The n-side strips are isolated by  $p^+$  strips to avoid resistive coupling through the electron accumulation layer. The ohmic resistance of the accumulation layer is used to bias the  $n^+$ -strips. A suitable shape of the blocking-strips at the strip ends allows effective biasing with resistances in the range of a few  $\text{M}\Omega$ . The  $n^+$  implant strip pitch is  $50 \mu\text{m}$  and the readout pitch is  $100 \mu\text{m}$ .

The depletion voltage of the detectors ranges between  $15\text{V}$  and  $40\text{V}$ . The detectors were operated at a voltage about 50% above depletion. Because the capacitor chips are not high voltage proof the front end electronics is operated at bias voltage; p-side on ground potential, n-side on  $V_{\text{Bias}}$ . Bipolar transistors used as level shifters transfer the analog output signals at bias potential down to the output amplifier sitting at ground potential. All digital control signals are transferred via fast opto-couplers.

The VIKING front-end chip is a low power, low noise, 128 channel CMOS readout chip [7]. Each channel consists of a charge sensitive amplifier, a bandwidth limiting CR-RC shaper and a sample/hold unit. The analog output is multiplexed, clocked at a maximum speed of  $20 \text{ MHz}$  (according to ref. [7]). In this setup we have operated the VIKING-chip at a speed of  $625 \text{ kHz}$  only. Using a shaping time of  $1.5 \mu\text{s}$  gives the equivalent noise charge of [7]:

$$ENC = 125 e^- + 14.4 e^- \cdot C_{\text{IN}}(\text{pF}).$$

Each detector is connected to four VIKING-chips on each side, defining the total sensitive area to be  $512 \times 512$  strips or  $25.6 \times 51.2 \text{ mm}^2$ .

To minimize the number of external control signals from the main sequencer, and to minimize pick-up the actual timing and control signals for the VIKING-chips are generated by local FPGA-chips [9] located on the front-end hybrids, which are steered with four external signals.

The amplification of the analog output signals, the generation and distribution of the control signals and low-voltage regulation are handled on the interconnect card, also mounted inside the detector unit frame.

Figure 3 shows the analog readout chain. The differential analog output signals are shifted to the same voltage level, amplified and finally digitized and stored in the FADCs. All 1024 channels of one detector unit are read out serially, and the four detector units in parallel.

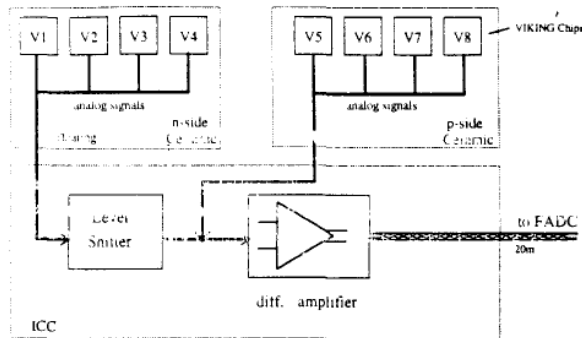


Figure 3: The analog output chain.

### 3 Data acquisition

The data acquisition system is based on the online system SPIDER developed at CERN [10] for such applications. SPIDER is a skeleton of four independent processes and a buffer manager written in C for a MVME-167-CPU (Motorola 68040) running OS-9. The four main tasks with respect to the telescope operation are:

1. **the producer:** This process controls the VME-system, reads out the four 10-bit FADCs and copies the raw data into the SPIDER circular buffer. The raw data block of an event is 8 kB, two bytes for each of the 4096 strips.
2. **the analyser:** The analyser receives a small fraction of events for monitoring. A copy of the raw data block is sent to a workstation for further analysis.
3. **the recorder:** Each event reaching the circular buffer is written to tape (EXABYTE) and thereafter deleted from the buffer.
4. **the controller:** The user interacts with the controller to adjust parameters for the data acquisition. This process provides the communication between all SPIDER-tasks and manages the circular buffer.

Using a low density EXABYTE tape (type 8200)<sup>1</sup> and continuous data taking the achievable event rate with no data reduction is 30 Hz. In pulsed beams up to 60 events per second can be recorded. Some online displays are available on a local OS-9 terminal:

**hits:** four two-dimensional distributions of all hits seen by the analyser ,

**pulseheights:** landau distributions of the pulse heights for each detector side,

<sup>1</sup>the write density is in the order of 300 kByte per second

**pedestals:** the ADC values for all strips in absence of hits,

**noise:** the variance of the ADC values in pedestal-events for each single strip.

## 4 Data analysis

The main tasks of the offline analysis are the cluster selection, the position reconstruction of hits on an individual detector in its local frame, the relative alignment of the four detector stations with respect to each other and the track definition of particle tracks through the telescope. To illustrate the different parts of the analysis procedure example plots for a testbeam setup as shown in figure 1 are given.

### 4.1 Cluster selection

Each raw event consists of 4096 ADC values, one for each strip. After pedestal correction a coherent noise fit is applied for each VIKING group (128 strips) consisting of a constant term and a (moderate) slope as observed in the raw data. Both values are fitted twice for each event including only *good* channels in both fits. For the second fit strips with particle hits are removed. The classification of strips as *good*, *noisy* and *dead* uses their noise values relative to some thresholds. Strips with a noise value above 3.5 times the average noise are flagged as *noisy*. Noise values below 0.2 times the average indicate *dead* strips. All other strips are flagged as *good*. The average noise values  $\sigma_{\text{mean}}$  are calculated for each VIKING from the *good* strips.

Noise values, pedestals and classification flags are updated after ten pedestal events. Strips with a charge value of at least eight times the noise value of that strip and with the correct sign (positive on *p*-sides and negative on *n*-sides) are called a 'hit'. Fig. 4 shows a typical charge distribution for a hit on both sides of a detector. Hit strips define seeds for the building of clusters consisting of the neighbouring strips. The expansion of a cluster to the left (right) stops, if the absolute value of the charge of the strip to be included falls below the lower threshold (4 times its noise value). For each cluster the 'main' channel with the largest absolute charge value and four neighbour strips (two to the left and two to the right), the sum of all charges and the width and position of the cluster are stored for the position reconstruction. Fig. 5(a) shows the average noise for strips on the junction side and fig. 5(b) gives the distribution of the cluster signal to noise value on the same side.

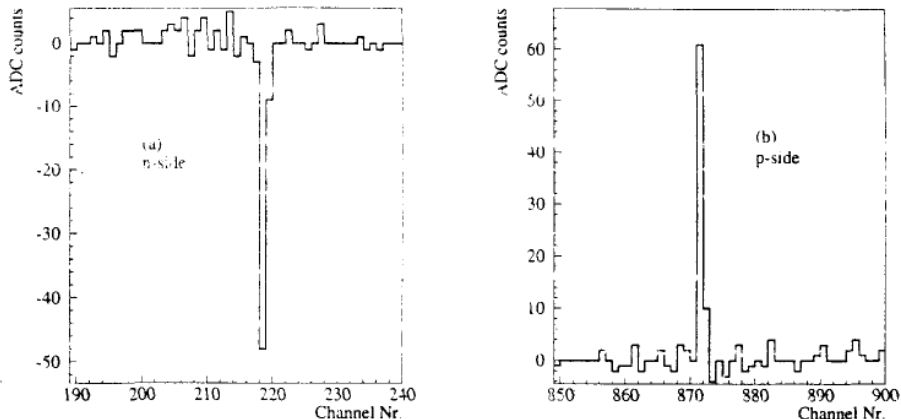


Figure 4: A typical charge distribution for a hit after pedestal corrections seen on both sides of the detector

## 4.2 Position reconstruction

The reconstruction of the intercept of a minimum ionising particle is done using the  $\eta$ -algorithm [11]. A minimum ionising muon typically deposits charge on two adjacent strips. The pulse heights of these two strips are  $p_L$  for the left and  $p_R$  for the right strip. The quantity  $\eta$  defined as

$$(1) \quad \eta = \frac{p_L}{p_L + p_R}.$$

should be distributed symmetrically around the value 0.5 if the incoming particles uniformly illuminate the area covered by adjacent strips. After applying a charge correction,  $\eta$  distributions as shown in fig. 6(a) are observed. The integrated distribution of  $\eta$  returns the particle position between the two strips selected for a particular value of  $\eta$  (fig. 6(b)):

$$(2) \quad x(\eta) = x_R - \frac{\Delta x}{N_0} \int_0^\eta d\eta' \frac{dN}{d\eta'}.$$

where  $x_R$  is the absolute position of the right strip,  $\Delta x$  the readout pitch and  $N_0$  the number of events included in the distribution. The integrated  $\eta$ -distributions are evaluated separately for each detector side.

Next, the position measurements on both sides of a detector are combined to achieve a two dimensional readout. Even in cases of multiple hits the correct combinations of  $n$ - and  $p$ -side clusters can be found because the absolute values of cluster charges on both sides are proportional, so that the clusters with the largest charge belong together and so on. Fig. 7 displays the correlation obtained between cluster charges on  $n$ - and  $p$ -sides of a detector. On each detector the hits are now given in the local detector reference frame.

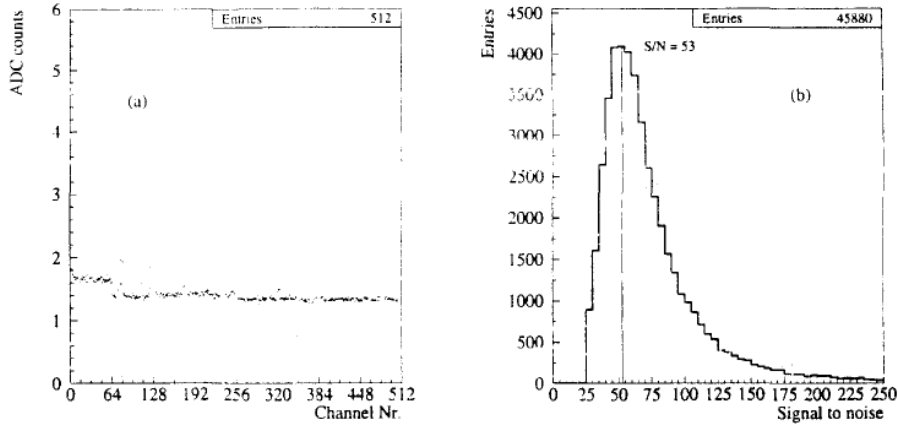


Figure 5: (a) Average noise values on the junction side of one detector (an ADC count corresponds to  $\sim 315$  electrons  $ENC$ ); (b) distribution of signal to noise (junction side).

### 4.3 Relative alignment

To align the detector stations with respect to each other we adopt an outer reference system defined by the local system of the detector no. 4 with  $x$  and  $y$  running along the strip directions and  $z$  perpendicular to the detector plane in beam direction. The positions of the other three detectors in this system are described by an offset vector  $\mathbf{v}^i$  ( $i = 1, 2, 3$ ) moving the center of a detector unit, an angle  $\Phi^i$ , describing a rotation of the detector in the  $xy$ -plane and two angles  $\Theta_x^i$  and  $\Theta_y^i$  for rotations in the  $yz$ - and the  $xz$ -plane.

In the testbeam setup of fig. 1 with a beam divergence as small as  $200 \mu\text{rad}$  the telescope is very sensitive to all movements in directions orthogonal to the beam direction. Therefore  $\mathbf{v}_x^i$ ,  $\mathbf{v}_y^i$  and  $\Phi^i$  are the most important quantities to determine. They can be calculated with very good accuracy while in  $z$ -direction a position uncertainty of up to  $0.5 \text{ mm}$  can be tolerated. The  $z$ -positions were therefore determined using an standard optical method. The relative transverse orientations of the modules are obtained from the data itself using an iterative method applied to two dimensional residual distributions. The residuals for the  $i$ -th detector in  $x$ -direction are defined as the difference between the measured  $x$ -coordinate  $X_i$  and the calculated  $x$ -coordinate  $X'_i$  at the position of detector  $i$  obtained from the resolution weighted measurements of the other three detectors. The  $y$  direction is treated accordingly.

After fitting straight lines to the distributions  $X_i - X'_i$  vs.  $X_i$  ( $Y_i - Y'_i$  vs.  $Y_i$ ) and  $X_i - X'_i$  vs.  $Y_i$  ( $Y_i - Y'_i$  vs.  $X_i$ ) deviations from zero of the intercepts leads to corrections of  $\mathbf{v}_x^i$  ( $\mathbf{v}_y^i$ ) while deviations from zero of the slopes allow corrections in  $\cos \Theta_y^i$  ( $\cos \Theta_x^i$ ) and  $\sin \Phi^i$

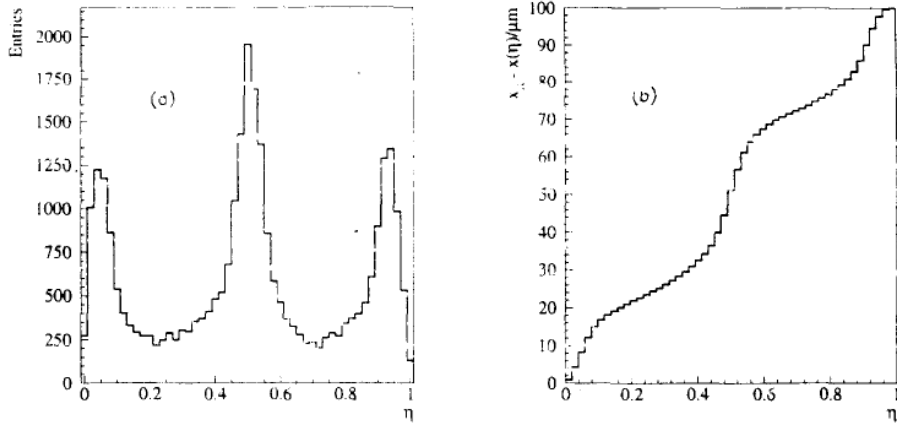


Figure 6:  $dN/d\eta$ -distribution on the ohmic side (a); the derived distance of the intercept to the right strip from the integrated distribution normalized to the number of events and the readout pitch (b)

$(-\sin \Phi^i)$ . An optimal set of values is found if all intercepts and slopes of all distributions vanish within errors.

The statistical uncertainties of the optimum parameters are given in table 1 for 10.000 events with a single hit on all four detectors. Manufacturing imperfections regarding the orthogonality of the two silicon detector sides and surface deformations are found to be in the order of 0.2mrad and  $20 \mu\text{m}$  respectively. Systematic uncertainties introduced hereby exceed the statistical errors on intercepts and slopes (see table 1).

Table 1: Alignment errors obtained from 10000 events. The statistical errors are given in the second column while the systematic uncertainties are shown in the third column

Parameter	Statistical errors	Observed shifts
$v_{x,y}$	$\pm 0.1 \mu\text{m}$	$\pm 0.2 \mu\text{m}$
$\Phi$	$\pm 0.02 \text{ mrad}$	$\pm 0.2 \text{ mrad}$
$ \Theta_{x,y} $	$\pm 1.3 \text{ mrad}$	—

#### 4.4 Spatial resolution

The residual distribution of the  $p$ -side of detector no. 4 is shown in fig. 8. The variances  $\sigma_{\text{res}_i}^2$  and  $\sigma_{\text{res}_i}^2$  of the residual distributions of the  $i$ -th detector depend on the intrinsic

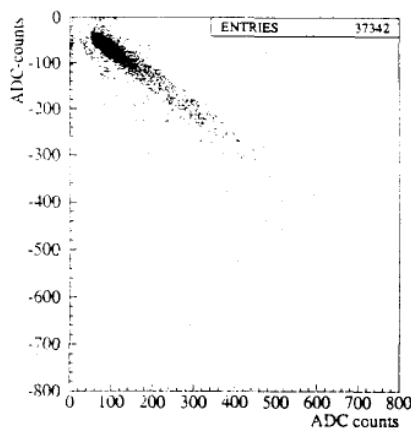


Figure 7:  $n$ -side cluster charges (vertical axis) vs.  $p$ -side cluster charges (horizontal axis) in ADC counts

Table 2: Intrinsic resolutions of the detector planes

Detektor	$\sigma_{\text{intr}} (\mu\text{m})$		$S/N$	
	$p$	$n$	$p$	$n$
1	8.0	8.0	37	32
2	2.9	5.9	43	32
3	3.9	4.8	37	37
4	2.7	6.0	53	37

Table 3: Intrinsic resolution of the telescope on the front face of the Si/W calorimeter.  $\sigma_c$  is the resolution of the intercept at the Si/W detector and  $\sigma_m$  the resolution of the slope of a particle trajectory

	$X$	$Y$
$\sigma_c (\mu\text{m})$	3.3	2.3
$\sigma_m (\mu\text{m}/\text{m})$	2.9	1.9

resolutions  $\sigma_{\text{intr}^i}$ , the error of the extrapolation of the track through the three other detectors  $\sigma_{\text{extr}^i}$ , and the track deviation due to multiple scattering  $\sigma_{\text{scatt}^i}$ :

$$(3) \quad \sigma_{\text{res}_z^i}^2 = \sigma_{\text{intr}_z^i}^2 + \sigma_{\text{extr}_z^i}^2 + \sigma_{\text{scatt}_z^i}^2.$$

The values for  $\sigma_{\text{res}}$  are in the range of  $5.6 \mu\text{m}$  to  $10.5 \mu\text{m}$ , detector dependent. Because the extrapolation errors depend on the resolutions of the three detectors involved their intrinsic resolutions are varied until equation (3) is selfconsistent for all eight detector planes. The results are given in table 2.

The combined intrinsic telescope resolution (for the setup in fig.1) is given by the extrapolation error of a weighted straight line fit using the individual detector resolutions as errors on the measured points. With the origin on detector no. 4 (mounted directly onto the front face of the test calorimeter) the values in table 3 are obtained.

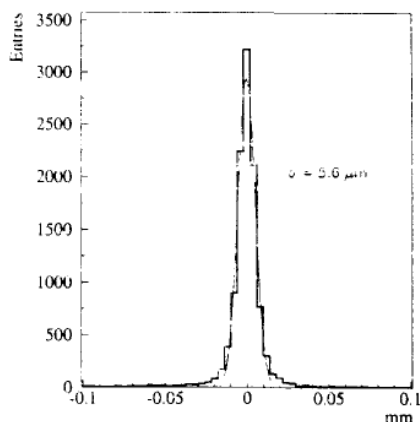


Figure 8: Residual distribution for the junction side of detector no. 4

## 5 Summary

We have built and used a beam telescope consisting of four double sided microstrip detectors in a 70 GeV  $\mu^-$  beam at CERN. The telescope, its readout electronics and the data acquisition system is operated stand alone. We have observed signal to noise values of 53 and 37 on  $p$ - and  $n$ -side of the best detector planes, respectively. In telescope operation slope and intercept of a particle trajectory on the front face of a test calorimeter are measured to be

$$\sigma_m = 1.9 - 2.9 \mu\text{rad} \quad \text{and} \quad \sigma_{xy} = 2.3 - 3.3 \mu\text{m}.$$

## 6 Acknowledgements

We gratefully acknowledge the help obtained from M. Goodrick and P. Gällnö in providing and programming the FPGA-chips. We would like to thank W. Glessing, S. Gross and A. Eyring for providing substantial help on mechanical and electrical issues. We also like to thank the Si/W-group, in particular D. Kellogg, R. Lahmann, M. Mannelli, D. Strom and D. Wagner for their support.

## References

- [1] P. P. Allport et al., Nucl. Instr. and Meth. **A346**, (1994) 476;  
M. Acciarri et al., **CERN PPE 94-122** (1994);

- N. Bingevors et al., Nucl. Instr. and Meth. **A328** (1993) 447;  
 G. Batignani et al., Nucl. phys. B(Proc. suppl.) : 23A (1991) 291.
- [2] see for example: J. Straver et al., Nucl. Instr. and Meth. **A348** (1994) 485;  
 L. Labarga, et al., IEEE trans. nucl. sci. : 37 (1990);  
 R. Bailey, et al., Nucl. Instr. and Meth **A226** (1984).
- [3] S. Menke, Diploma Thesis, Bonn **IB-94-35** (1994);  
 B. A. Raith, Diploma Thesis, Bonn **IB-94-36** (1994).
- [4] Motorola Inc., Computer Group.
- [5] LEPSI Development Strasbourg, VME module Sirocco, W. Dulinski et al. (1992), unpublished.
- [6] The OPAL Collaboration, CERN/LEPC 91-8 LEPC/M-100 (1991);  
 B. Anderson et al., IEEE Trans. Nucl. Sci., 41 no. 4 (1994) 854.
- [7] E. Nygard et al., Nucl. Instr. and Meth. **A301**, (1991) 506;  
 R. Brenner et al., Proc. of the 6th European Symposium on Semiconductor Detectors, Milano, Italy, Febr 1992;  
 O. Toker et al., Nucl. Instr. and Meth. **A340**, (1994) 572.
- [8] CSEM Neuchatel (CH);  
 M. Caria et al., **INFN/AE-94/05** (1994).
- [9] M. Goodrick, OPAL-Technical Note **TN231** (1994);  
 P. Gällnö, OPAL-Technical Note **TN255** (1994).
- [10] Y. Perrin et al., SPIDER, User's Guide, CERN preprint (1991).
- [11] E. Belau et al., Nucl. Instr. and Meth. **A214** (1983) 253.

